crystals

MDPI

Article

Hydrogen Bonding in Crystals of Pyrrol-2-yl Chloromethyl Ketone Derivatives and Methyl Pyrrole-2-Carboxylate

Małgorzata Domagała [1,*], Alina T. Dubis [2], Sławomir Wojtulewski [2], Manfred Zabel [3] and Arno Pfitzner [3]

[1] Faculty of Chemistry, University of Łódź, Pomorska 163/165, 90236 Łódź, Poland
[2] Faculty of Chemistry, University of Białystok, Ciołkowskiego 1K, 15245 Białystok, Poland
[3] Institute of Inorganic Chemistry, University of Regensburg, 93040 Regensburg, Germany
* Correspondence: malgorzata.domagala@chemia.uni.lodz.pl

Abstract: The crystal and molecular structure of three derivatives of carbonyl 2-substituted pyrroles was determined by the single crystal X-ray diffraction. There are 2,2-dichloro-1-(1-methyl-1*H*-pyrrol-2-yl)ethan-1-one (**I**), 2-chloro-1-(1*H*-pyrrol-2-yl)ethan-1-one (**II**) and methyl 1*H*-pyrrole-2-carboxylate (**III**). All compounds crystallize with one molecule in the asymmetric unit in $P2_12_12_1$ for **I** and **II**, and $P2_1/c$ group for **III**. Despite the similar structures of the investigated compounds, the hydrogen bonds formed in their crystal structures adopt different H-bond motifs. In structure **I**, the dimers $R_1^2(5)$ and $R_2^1(7)$ form a chain along the *b*-axis, while in structures **II** and **III**, chain C(5) structural motifs are formed. The *single point* calculations at a ωB97XD/6-311++G(d,p) level of theory indicate that systems with N-H···O bonds have greater interaction energies (are more stable) compared with systems featuring C-H···O/Cl bonds. A descriptive Hirshfeld analysis showed that the greatest differences are visible for the H···H interactions. These H···H interactions predominate in structure **III**, accounting for 45% of the intermolecular interactions, while in structures **I** and **II**, they account for only 25%. Although compounds **I-II** contain Cl-atoms, the percentage of Cl···Cl interactions is rather low. In structure with two Cl-atoms (**I**), the contribution of the Cl···Cl contacts is 8.7% and for **II**, the contribution accounts for only 0.4% of the interactions.

Keywords: crystal structure; hydrogen bond; Hirshfeld surface; pyrrol -2-yl ketone; DFT

Citation: Domagała, M.; Dubis, A.T.; Wojtulewski, S.; Zabel, M.; Pfitzner, A. Hydrogen Bonding in Crystals of Pyrrol-2-yl Chloromethyl Ketone Derivatives and Methyl Pyrrole-2-Carboxylate. *Crystals* **2022**, *12*, 1523. https://doi.org/10.3390/cryst12111523

Academic Editors: Kil Sik Min, Lilianna Checinska and Magdalena Małecka

Received: 11 October 2022
Accepted: 22 October 2022
Published: 26 October 2022

1. Introduction

Five-membered heterocyclic compounds are among the most widespread and important building blocks of molecular structures. Among them, the pyrrole ring, which is a building element in many natural products, such as hem [1], chlorophylls [2], and bioactive alkaloids [3–7], is the most common. Although the parent pyrrole has been characterized experimentally [8] and analyzed [9–12] by theoretical methods, relatively little is known about its derivatives, particularly the noncovalent governing of the crystal structure of this class of compounds.

Although some studies have been devoted to 2-substituted pyrroles, [13] mainly to assess the conformational preferences [14–19] or aromaticity [20–22], there is still a lack of certain knowledge about noncovalent interactions of pyrrol-2-yl-carbonyl compounds. However, general studies show that intermolecular interactions strongly influence the arrangement of molecules in crystals, especially directional hydrogen bonds [23,24].

Halogen bonds also impart directionally in crystal structures, and may be considered as counterparts of hydrogen bonds [25–31]. Halogen bonds involving C-Cl···O have been observed in the crystal structure of 1-methylpyrrol-2-yl trichloromethyl ketone [32]. Analyses of other interactions of carbonyl 2-substituted pyrroles show mainly different kinds of hydrogen bonds [16–19,32]. Density Functional Theory (DFT) calculations indicated that for the *s-cis* conformation of pyrrole-2-carboxylic acid, where the NH and COO bonds are located on the same side of the moiety, two centrosymmetric dimers are possible [33].

For each dimer, there are two equivalent hydrogen bonds, two O-H···O bonds creating $R_2^2(8)$ motifs according to Etter's rules [34,35] or two N-H···O hydrogen bonds forming $R_2^2(10)$ motifs.

H-bonded motifs in crystal structures are described by graph set assignments [34,35]. R denotes the ring, and the number of atoms that make up the ring is given in parentheses. Therefore, for $R_2^2(8)$ there are eight ring atoms linked through covalent and hydrogen bonds, since two hydrogen bonds form between two carboxylic groups. The superscript and subscript denote the number of proton acceptors and proton donors, respectively. For $R_2^2(8)$ there are two equivalent proton acceptor O centers (since the dimer is linked through two equivalent molecules) and two equivalent proton-donating bonds (OH). Etter also described other motifs [34,35]: C denotes the chain of atoms containing hydrogen bonds which repeat in the crystal structure, S refers to intramolecular hydrogen bonds and D replays to a dimer where a single hydrogen bond exists.

In the case of the *s-trans* conformer of pyrrole-2-carboxylic acid, there is only the possibility that the dimer contains two equivalent O–H···O bonds within the $R_2^2(8)$ motif. An X-ray structure analysis confirmed that pyrrole-2-carboxylic acid forms crystals with *s-cis* conformers that form the motifs $R_2^2(8)$ and $R_2^2(10)$ mentioned above [19]. Recently, 2-pyrrolecarboxylic acid and 1-methyl-2-pyrrolecarboxylic acid have been studied by thermochemical measurements and computational analyses [36], and pyrrole-2-carboxamide has been analyzed by spectroscopic and X-ray methods, and DFT calculations [19]. For the latter compound, the *s-cis* conformer was revealed and the presence of centrosymmetric dimers in crystals connected through N–H···O bonds.

Due to the importance and prevalence of pyrrole compounds in organic chemistry, we have conducted research aimed at extending knowledge of the structural properties in some pyrrol-2-yl carbonyl compounds, particularly focusing on the role of the intermolecular interactions in their crystal structures. When searching the Cambridge Structural Database [37], we found more than 26,500 compounds containing pyrrole rings. Among them, there are almost 930 structures with a 2-substituted pyrrole core and only 153 with a 2-pyrrol-2-yl core, and 14 of the 27 pyrrol-2-yl halogenated ketone contain a chlorine atom.

2. Materials and Methods

2.1. Synthesis of Pyrrol-2-yl Chloromethyl Ketones

The conventional Friedel–Crafts acylation method was applied for the preparation of aromatic ketones **I** and **II** (Scheme 1) [38]. The title pyrroloketones were generally obtained using acid chlorides as acylating agents and stoichiometric amounts of $AlCl_3$ as a reaction promoter. Dichloroacetyl chloride or chloroacetyl chloride (0.02 mol) was dissolved in 10 mL of anhydrous ethyl ether and 0.02 mol of $AlCl_3$ was added. Then, the 0.02 mol of freshly distilled pyrrole was added dropwise and the reaction mixture was stirred for one hour at room temperature. After that time, an aqueous solution of potassium carbonate (0.02 mol) was added. The resulting mixtures were extracted twice with ether and the crude products were purified by crystallization from hexane. Spectroscopic data are available in [39].

2.2. Synthesis of Methyl Pyrrole-2-Carboxylate

Methyl pyrrole-2-carboxylate (**III**) was synthesized (Scheme 2) according to the method of Bailey et al. [40]. Sodium (0.08 g) was dissolved in 50 mL of anhydrous methanol, and 5.3 g (0.025 mol) of pyrrol-2-yl trichloromethyl ketone was added portion by portion over a 10-minute period. The solution was stirred for 30 min and then concentrated to dryness using a rotary evaporator. The oil residue was partitioned between ethyl ether and 3M HCl (1:1, V:V). The ether layer was separated, and the aqueous layer was washed once with ether. The combined ether solutions were washed once with an aqueous sodium hydrogen carbonate solution (10%), dried with magnesium sulfate, and concentrated by distillation. The crude products were purified by crystallization from a mixture of hexane and ethyl acetate (1:1; V:V), giving 2.5 g of ester. Spectroscopic data are available in [16,17].

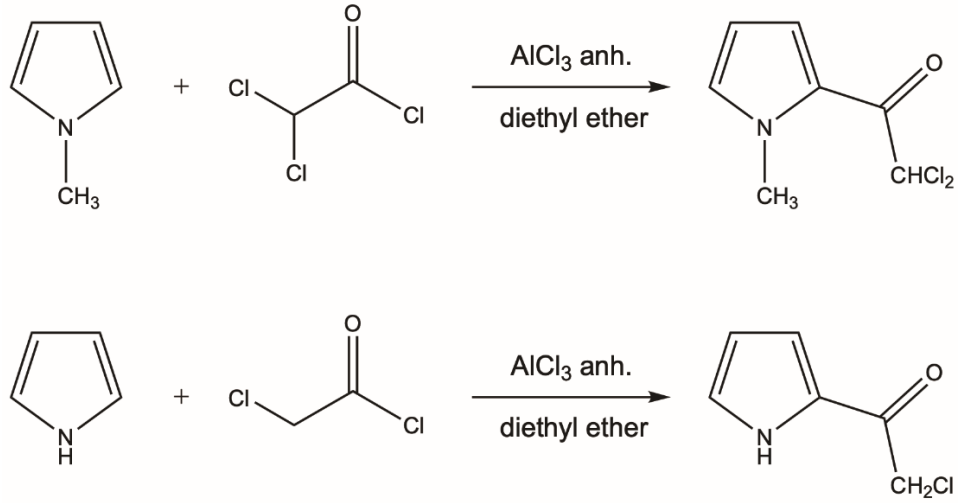

Scheme 1. Reaction scheme of **I** (top) and **II** (bottom).

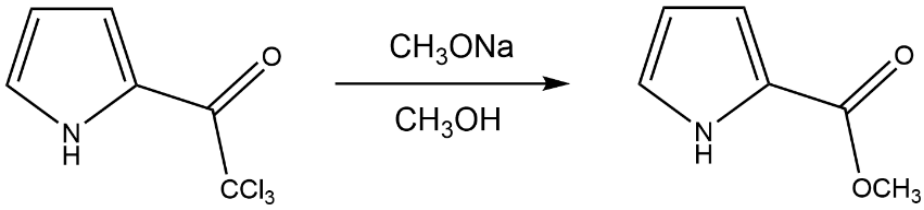

Scheme 2. Reaction scheme of **III**.

2.3. X-ray Diffraction Analysis

Measurements of structure **I** was performed on a Stoe IPDS diffractometer with graphite monochromated MoKα radiation (λ = 0.71073 Å). For the compound, data reductions were performed with Stoe IPDS [41]. The intensities were corrected for Lorentz and polarization effects. An empirical absorption correction was applied for compound **I** [42]. The structures of **II** and **III** were measured on Rigaku SuperNova Dual Source diffractometer, also with MoKα radiation (λ = 0.71073 Å). For both compounds, analytical absorption corrections were applied [43]. The data collection and refinement parameters are given in Table 1, and the structures of the molecules are shown in Figure 1. The structure was solved by direct methods with SIR-97 [44] for structures **I** and by SHELXS [45] for structures **II** and **III**, which revealed the positions of all non-H-atoms. Non-H-atoms were refined anisotropically. For structure **I**, all of the H-atoms were located in a difference electron density map, whereas for structures **II** and **III**, they were placed in geometrically calculated positions. Then, for all structures, positions of H-atoms were allowed to refine together with individual isotropic temperature factors. The refinement of each structure was carried out on F^2 using full-matrix least-square procedures, which minimized the function $\sum w(F^2_o\text{-}F^2_c)^2$ with SHELXL-2014/7 [46]. Geometry analysis and molecular plots were obtained using the PLATON program [47] and Mercury [48].

Crystal data for **I**, $C_7H_7Cl_2NO$ (M = 192.04 g/mol): orthorhombic, space group $P\,2_12_12_1$ (no. 19), a = 5.8789(2) Å, b = 7.4029(2) Å, c = 14.6418(4) Å, V = 860.05(14) Å^3, Z = 4, T = 123.0(1) K, μ(MoKα) = 0.694 mm^{-1}, Dcalc = 1.483 g/cm^3, 10,785 reflections measured (3.566° ≤ Θ ≤ 27.918°), 2030 unique (Rint = 0.0328), which were used in all calculations. The final R1 was 0.0255 [$I > 2\sigma(I)$] and $wR2$ was 0.0671 (all data).

Crystal data for **II**, C_6H_6ClNO (M = 143.57 g/mol): triclinic, space group $P\,2_12_12_1$ (no. 19), a = 5.8789(2) Å, b = 7.4029(2) Å, c = 14.6418(4) Å, V = 637.22(3) Å^3, Z = 4, T = 100.0(2) K, μ(MoKα) = 0.504 mm^{-1}, Dcalc = 1.496 g/cm^3, 3887 reflections measured (2.782° ≤ Θ ≤ 27.773°), 1404 unique (Rint = 0.0428), which were used in all calculations. The final R1 was 0.0333 [$I > 2\sigma(I)$] and $wR2$ was 0.0743 (all data).

Crystal data for **III**, $C_6H_7NO_2$ (M = 125.13 g/mol): monoclinic, space group $P\,2_1/c$ (no. 14), a = 7.5448(2) Å, b = 5.4641(1) Å, c = 14.7330(3) Å, β = 100.419(2)°, V = 597.36(2) Å^3, Z = 4, T = 100.0(2) K, μ(MoKα) = 0.106 mm^{-1}, Dcalc = 1.391 g/cm^3, 6625 reflections measured (2.745° ≤ Θ ≤ 27.854°), 1358 unique (Rint = 0.0397), which were used in all calculations. The final R1 was 0.0443 [$I > 2\sigma(I)$] and wR2 was 0.0947 (all data).

CCDC 2120675–2120677 contains the supplementary crystallographic data for this paper. These data can be obtained free of charge via http://www.ccdc.cam.ac.uk/conts/retrieving.html (accessed on 21 October 2022) (or from the CCDC, 12 Union Road, Cambridge CB2 1EZ, UK; Fax: +44 1223 336033; E-mail: deposit@ccdc.cam.ac.uk).

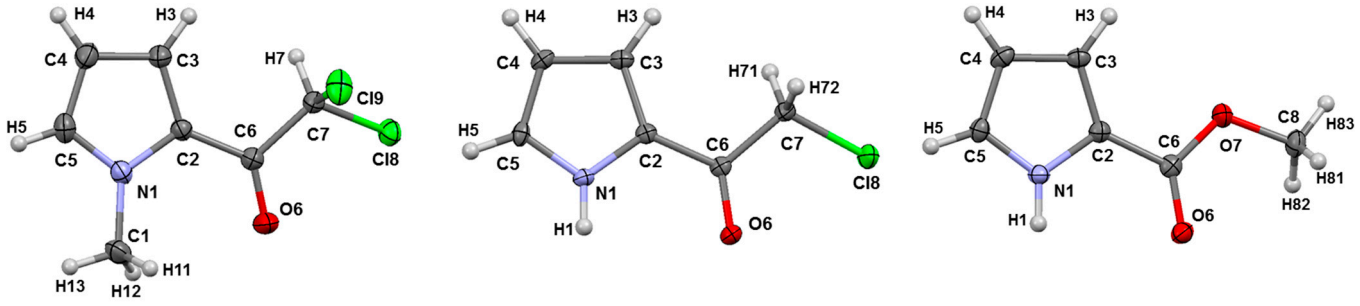

Figure 1. Molecular structures of (**a**) 2,2-dichloro- 1- (1-methyl-1H- pyrrol- 2-yl)ethan-1-one (**I**), (**b**) 2-chloro-1-(1H-pyrrol-2-yl)ethan-1-one (**II**) and (**c**) methyl 1H-pyrrole-2-carboxylate (**III**). Atomic displacement ellipsoids are drawn with a 50% probability level.

2.4. Hirshfeld Surface Analysis

Hirshfeld analysis was performed using Crystal Explorer [49,50]. The Hirshfeld surface maps intermolecular contacts, and it is computed at the sum of d_e and d_i, the distances from the external atoms to the surface and the internal atoms to the surface, respectively [49]. Sums of distances shorter than the sum of the van der Waals radii of two neighboring atoms are marked with red spots, distances close to the van der Waals radii are marked in white, and distances larger than the sum of van der Waals radii are marked in blue. A qualitative description of all relevant contacts in the crystal structure is shown in fingerprint graphs [50] by plotting the distances from contact atoms to the Hirshfeld surface, d_i and d_e, in a 2D graph, creating a 'heatmap' of noncovalent interactions.

2.5. Full Interaction Maps Analysis

The Full Interaction Maps feature is included with mercury [48]. This tool generates a picture of the interaction landscape of a molecule from its 3D coordinates. Using statistical distributions from structures included in the CSD, it predicts the most likely locations for a variety of functional groups. By comparing this distribution with a 3D packing diagram, it can determine whether a crystal structure fulfils the desired interactions of a particular conformation of a particular molecule.

2.6. Theoretical Calculations

All molecular systems were examined using the ωB97XD [51] variant of DFT with the 6-311++G(d,p) base set [52–55]. This level of theory gives good results in the case of hydrogen bonds or other weak interactions with the contribution of dispersion effects, and is appropriate for the calculation of relatively large systems [56,57]. All three systems (**I-III**) were calculated with use of *single point* calculations in geometries taken from the crystal state. Only the positions of H-atoms were normalized according to neutron diffraction data [58], which is a standard procedure for model system in geometries extracted from X-ray experiments. All calculations were carried out using the Gaussian09 package (revision D.01) [59]. Interaction energies for the analyzed systems have been computed as the

difference between the total energy of the complex and the energies of monomers, and were corrected for the basis set superposition error (BSSE) using the counterpoise procedure [60]. The monomers were in the same geometries as those in a dimer complex or chain system; thus, we exclude the deformation energy from our consideration.

3. Results and Discussion

In a recent study, we investigated centrosymmetric dimers formed by pyrrol-2-yl chloromethyl ketones in their *s-cis* conformers [39]. According to current knowledge [20,61], the *s-cis* conformer, in which the NH and COO groups are located on the same side of the moiety, is more stable than the *s-trans* conformer. Theoretical calculations and crystal structure data show that, in general, the carbonyl group lies in the same plane as the pyrrole ring [17,19]. It is worth noting that the flat arrangement of the carbonyl group with respect to the pyrrole ring favors the formation of centrosymmetric dimers with two equivalent N-H$\cdots$O hydrogen bonds.

Spectroscopic and theoretical research on the conformations and intermolecular interactions of pyrrol-2-yl chloromethyl ketones and their N-methyl derivatives [39] show that the weakest hydrogen bond exists in the dimer of the pyrrol-2-yl trichloromethyl ketone, while the dimers of chloromethyl and dichloromethyl ketones have stronger hydrogen bonds, all of which are comparable in strength. All investigated pyrrol-2-yl chloromethyl ketones created the $R_2^2(10)$ motif [34,35] containing two equivalent hydrogen bonds N-H$\cdots$O. It is interesting that such motifs were barely sensitive to the number of Cl-atoms. It seems that the rigid skeletons of the pyrrole rings hamper the π-electron delocalization within the above-mentioned motif, and thus, the influence of the strength of the Cl substituents on the N-H$\cdots$O hydrogen bond strength was restricted for the pyrrol-2-yl chloromethyl ketones. On the other hand, X-ray investigations on 1-methylpyrrol-2-yl trichloromethyl ketone [32] show that in this structure, there is no centrosymmetric dimer motif, but two kinds of interactions are responsible for the arrangement of molecules in a crystal structure, C-H$\cdots$O and C-Cl$\cdots$O. The O-atom of the carbonyl group acts as an acceptor in both the hydrogen and halogen bond.

To extend this study, we investigated two pyrrol-2-yl chloroketones and one methyl pyrrole-2 carboxylate structures by single-crystal XRD analysis. According to this study, all the compounds crystallize with one molecule in the asymmetric unit and all show s-cis conformations, as depicted in Figure 1. Compound **III** crystallizes in the $P2_1/c$ centrosymmetric groups, while the other two compounds (**I** and **II**) crystallize in the $P2_12_12_1$ space group. This is reflected in the hydrogen bond motifs that are formed in the structures of these compounds. A ring motif of H-bonds [34,35] is present in the structures of **I**, and forms between the chain motifs in **III**.

3.1. XRD Analysis

The molecular crystal structures of compounds **I**, **II** and **III** were examined in terms of the geometric relationship between the pyrrole ring and carbonyl group. The structural variation of the three pyrrolylketones was ensured by the different numbers of halogen atoms or the methyl group substituted to the N atom from the pyrrole ring. Their structural overlay is shown in Figure 2.

All of the investigated compounds **I-III** have a flat pyrrole ring in their structure. The C6 carbonyl carbon atom deviates from the best plane calculated for the rings atoms N1-C2-C3-C4-C5 (Cg1) of −0.079(2)Å, 0.054(2)Å and 0.002(2)Å and oxygen atom O6 of −0.035(2)Å, 0.10(2)Å and −0.56(2)Å for structures **I**, **II** and **III, respectively**. Comparing the values of selected geometric parameters listed in Table S1, it can be seen that both the bond lengths and the valence angles show no significant differences between the compounds. To verify the geometric parameters, a Cambridge Structural Database search [37] was performed, from which 15 structures most resembling the investigated ketones and 11 structures corresponding to carboxylic acid were found. One of the esters found (Refcode DUCYOQ, [62]) is identical to the structure of **III** examined here. Although the geometry

of both structures is essentially identical, we decided to include structure **III** in this study since its structure was measured at a lower temperature, giving a better figure of merit for structure refinement. We also found structure **I** (Refcode UHIQEJ, [63]), but there is no structure description included in the cited work, so we decided to use our own data. The search schemes for fragments of molecules and the geometry parameters are given in Schemes S1 and S2 and Tables S3–S6. Figures S2 and S3 present a graphical representation [64] of the structures found in CSD. The values of all the geometrical parameters of the investigated compounds are comparable with those found in the CSD.

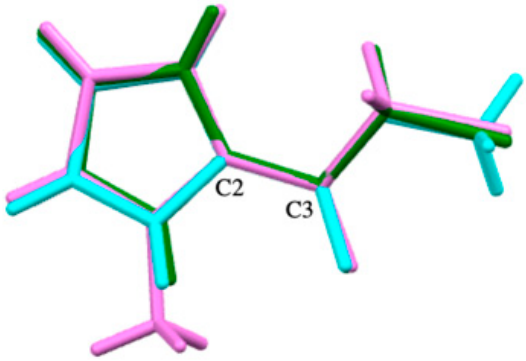

Figure 2. Structural overlay of molecular structures for all compounds in stick style (lavender color denotes **I**, green—**II**, blue—**III**).

The crystal packing analysis for the compounds investigated has revealed a variety of supramolecular architectures. The structure of the intermolecular interaction nets are guided by the presence of different types of H-bonds and stacking interactions. Despite the presence of the chlorine atoms in the structures, the classical halogen bond is not formed. The Cl atom either participates in hydrogen bonds as a proton acceptor for weak C-H donors, or in a C-Cl$\cdots\pi$ interaction.

The predictions of the most likely locations for a variety of functional groups (acceptors and donors) for the investigated compounds are presented on the full interaction maps (FIMs) [48] in Figure 3. The red regions of the maps denote areas that are identified as similar to a H-bond acceptor. The blue regions denote H-bond donors and the brown regions indicate hydrophobic groups. The FIMs of studied structures **I-III** show the expected directions for the formation of hydrogen bonds or others noncovalent interactions. The FIMs of studied structures **I-III** are shown in Figure 3 and Figure S1.

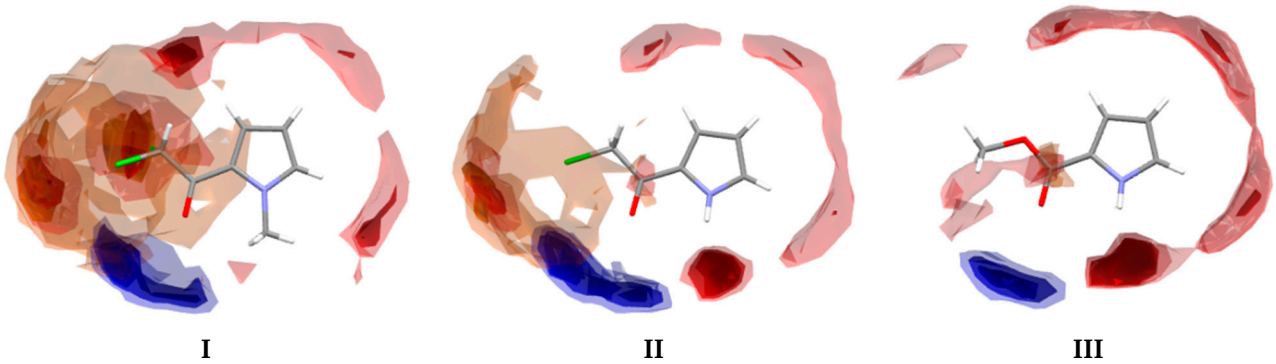

Figure 3. Full interactions maps for investigated compounds **I-III**.

In compound **I**, the carbonyl oxygen atom serves as a bifurcated acceptor in two C-H$\cdots$O interactions, giving an $R_2^1(7)$ motif. Additionally, the C-H as a bifurcated-donating group participates in a C-H$\cdots$Cl bond, forming the $R_1^2(5)$ motif. Both motifs create chains along **b**-axis. The chains form the C-H$\cdots\pi$ interaction, and create a zigzag 3D pattern, as shown in Figure 4. This structural motif is also stabilized by C-Cl$\cdots\pi$ interactions.

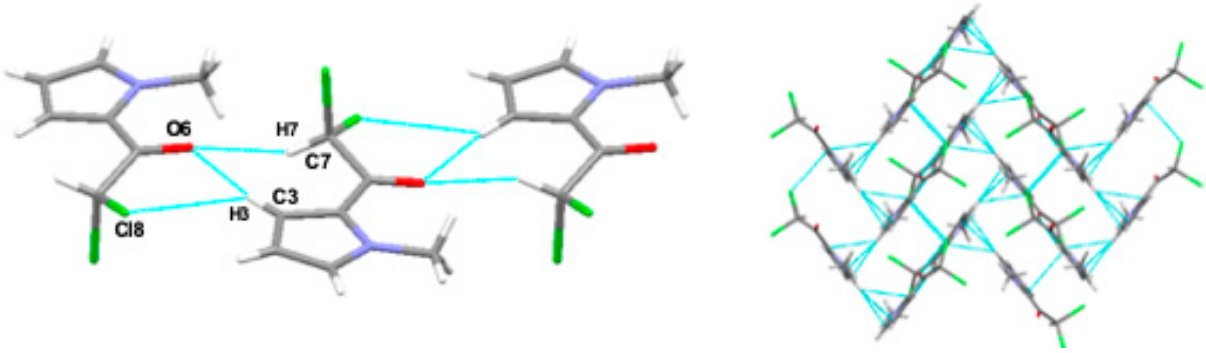

(**a**) (**b**)

Figure 4. Molecular arrangements in structure **I**. (**a**) **a**-axis view of the 1D chain created by C3-H3···O6, C3-H3···Cl8 and C7-H7···O6 H-bonds. H-bond parameters [C3-H3···O6] C3-H3 0.92(2)Å, H3···O6(1-x,−1/2−y,1/2+z) 2.50(2)Å, <C3H3O6 163(1)°, [C7-H7···O6] C7-H7 0.92(2)Å, H7···O6(1−x,−1/2−y,1/2+z) 2.94(2)Å, <C7H7O6 160(1)°, [C3-H3···Cl8] C3-H3 0.92(2)Å, H3···Cl8(1−x,−1/2−y,1/2+z) 2.94(2)Å, <C3H3Cl8 129(1)°, [C7-H7···O6] C7-H7 0.92(2)Å, H7···O6(1−x,−1/2−y,1/2+z) 2.330Å <C7H7O6 154°, (**b**) 3D arrangement viewed along the **b**-axis. Parameters of X/Y … Cg interactions [C5-H5···Cg1] C5-H5 0.96(2) Å, H5···Cg1 (−1/2+x,1/2−y,1−z) 2.57(2)Å, <C5H5Cg1 153(1)° and [C7-H7···Cg1] C7-H7 0.92(2) Å, H7 … Cg1 (1+x,y,z) 3.34(2)Å, <C7H7Cg1 100(1)°.

In structure **II**, the infinite chain along the **a**-axis is created by N-H···O hydrogen bonds, forming a C(5) chain motif (Figure 5). The molecule contains only one chlorine atom, which participates in H-bonding. The chain is stabilized by N-H···Cl and C-H···O interactions. Additionally, the 3D network is stabilized by C-H···π interactions.

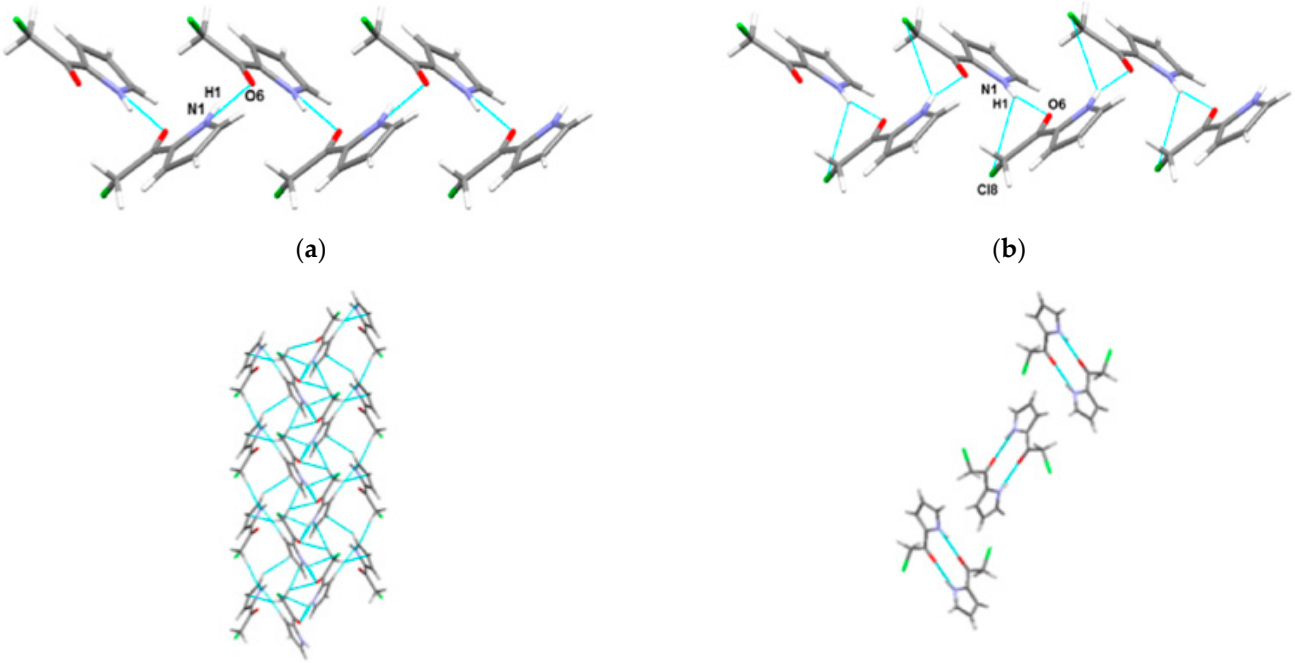

(**a**) (**b**)

(**c**) (**d**)

Figure 5. Molecular arrangements in structure **II**. (**a**) The **c**-axis view of the chain created by the hydrogen bond N1-H1···O6 and (**b**) stabilized by the hydrogen bonds N1-H1···Cl8 and C4-H4···O6. H-bond parameters [N1-H1···O6] N1-H1 0.90(2)Å, H1···O6(1/2+x,1/2-y,1-z) 2.05(2)Å, <N1H1O6 164(1)°, [C4-H4···O6] C4-H4 0.93(2)Å, H4···O6(3/2-x,1-y,−1/2+z) 2.52(2)Å, <C4H4O6 163(1)°,

[N1-H1···Cl8] N1-H1 0.90(2)Å, H1···Cl6(−1/2+x,1/2-y,1-z) 2.90(2)Å, <N1H1Cl8 126(1)°. (**c**) 3D arrangement viewed along the **c**-axis. Parameters of X···Cg interactions [C3-H3···Cg1] C3-H3 0.94(2) Å, H3···Cg1 (1-x,1/2+y,1/2-z) 2.72(2)Å, <C3H3Cg1 156(1)°. (**d**) 3D arrangement viewed along the **a**-axis.

The structure of the methyl pyrrole-2-carboxylate (**III**) is stabilized by N-H···O hydrogen bonds, which form the C(5) chain motif along the **b**-axis. The weak C-H···O interactions create centrosymmetric dimers between chains, giving the $R_2^2(6)$ motif. The 3D is additionally stabilized by C-H···π interactions (Figure 6).

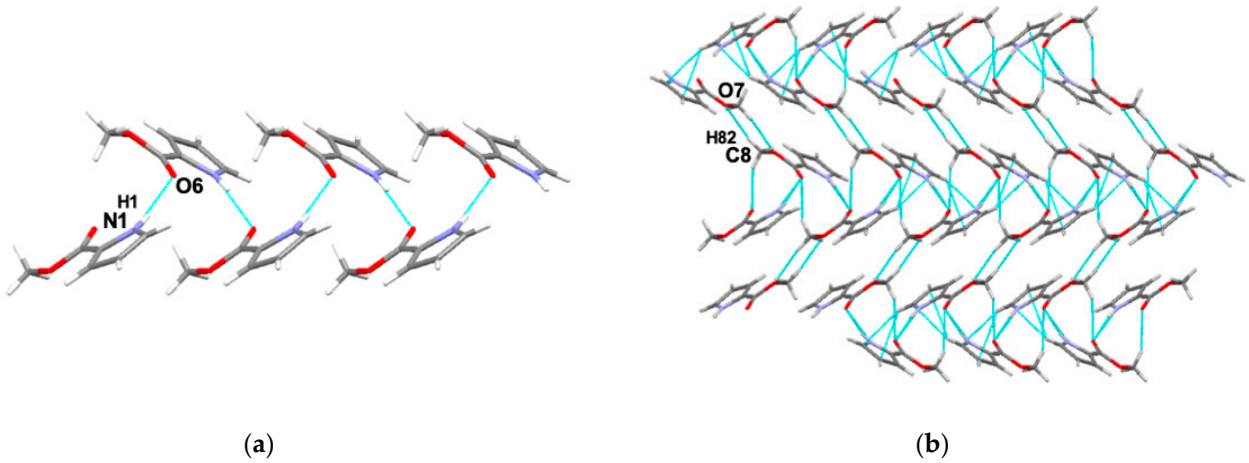

(**a**) (**b**)

Figure 6. Molecular arrangement in structure **III**. (**a**) An **a**-axis viewed chain of N-H···O. H-bond parameters [N1-H1···O6] N1-H1 0.88(2)Å, H1···O6(1-x,1/2+y,1/2-z) 2.06(2)Å, <N1H1O6 171(1)°. (**b**) View of the N-H···O chains connected by C-H···O hydrogen bonds and stabilized by C-H···π interactions. H-bond parameters [C8-H82···O7] C8-H82 0.97(2)Å, H82···O7(1-x,−1-y,1-z) 2.63(2)Å, <C8H82O7 156(1)°, [C5-H5···Cg1] C5-H5 0.95(2)Å H5···Cg1 (1-x,1/2+y,1/2-z) 2.64(2)Å, <C5H5Cg1 139(1)°.

3.2. Theoretical Calculations

Energy parameters from single point calculations were determined for the investigated H-bonded motifs found in the crystals of **I-III** using the ωB97XD/G-311++G(d,p) level of theory, and are given in Table 1. The positions of H-atoms were normalized according to neutron diffraction data [58]. Since the geometries of the studied molecules were taken from the crystal structures, the energy values apply to all possible interactions between the given molecules in each crystal.

Table 1. Selected geometric parameters and energy of interactions for two interacting molecules in crystal obtained at the ωB97XD/G-311++G(d,p) level of theory.

		D-H [Å]	H···A [Å]	<DHA[°]	E_{int}^{CP} [kcal/mol]	M.p. [°]
I	C7-H7···O6 C3-H3···Cl8	1.098 1.083	2.222 2.843	126 152	−7.62	65.8–66.5 [60]
II	N1-H1···O6 N1-H1···Cl8	1.030 1.030	1.919 2.828	163 124	−11.02	120.5 [60]
III	N1-H1···O6	1.030	1.917	170	−8.36	72

Looking at the obtained results, it can be seen that systems with the N-H···O bonds have greater interaction energies compared to those with C-H···O/Cl interactions.

The energy of a single interaction N-H···O in structure **III** is about 8.36 kcal/mol and is higher than the energy for centrosymmetric dimer motif optimized on the level of the

B3LYP/6-311++G(d,p) theory investigated earlier in [39] by more than 2 kcal/mol (dealing with a centrosymmetric dimer, we can divide the interaction energies in half for each of the two N-H···O bonds, and the energy of a single N-H···O bond was −6.63 kcal/mol). Such a difference may result both from the fact that for the interactions studied here, we chose single point calculations using the geometry from the crystal state, while previously, the optimization of the geometry was carried out and the B3LYP functional was used. Here, we used the ωB97XD functional because we noticed in our earlier research [56,57] that it gives results similar to those of the MP2 method. It should be noted that this functional contains Grimme's D2 numerical correction for dispersion effects [65]. Thus, additional effects included in the theory approximation may give a relatively larger interaction energy.

In structure **I**, the interaction energy is the lowest at 7.62 kcal/mol. This is expected since, in general, C-H is a relatively weaker donating group compared with O-H [66]. In the case of **I**, the nitrogen atom in the pyrrole ring is substituted with a methyl group, meaning that only weak H-bonds involving the C-H donor group may form, as opposed to the relatively stronger interactions with a N-H donor group.

In structure **II**, in addition to the N-H···O interactions, there is also the N-H···Cl interaction, a total interaction energy (for both mentioned interactions) is close to 11.02 kcal/mol. The calculations for the optimized dimer of this derivative showed that the energy of a single interaction was 6.34 kcal/mol [39]. However, the geometry of the system studied here, taken from experimental conditions, differs from the optimized dimer as it features a H-bond to Cl atom. Stronger H-bonding in the compound investigated here may therefore be associated with the additional interaction to the Cl atom.

It is worth mentioning that theoretically estimated interaction energies are in a straight relation with the physical macroscopic properties of the crystals. As it can be seen in Table 1, the melting points of studied crystals of pyrrolylketone derivatives are related to the estimated energies of interactions. The more negative value of $E_{\mathrm{int}}^{\mathrm{CP}}$, the higher the melting point.

3.3. Hirshfeld Surface Analysis

Figure 7 shows the Hirshfeld surfaces of the investigated compounds, showing red spots corresponding to contacts with a length shorter than the sum of van der Waals radii and white spots corresponding to contacts with a length equal to the sum of van der Waals radii. In the examined compounds **II** and **III**, the N1-H1···O6 interaction is the shortest distance in the hydrogen bridge, and thus, the strongest. For compound **I**, in which no H-bond involving an N atom is formed, there are three such short interactions. These are C3-H3···O6, C7-H7···O6 and C5-H5···π. Red spots on the Hirshfeld surface of **II** correspond to the N1-H1···O6 and C4-H4···O6 interactions. In the structure of **III**, there is also a short interaction, C5-H5···π.

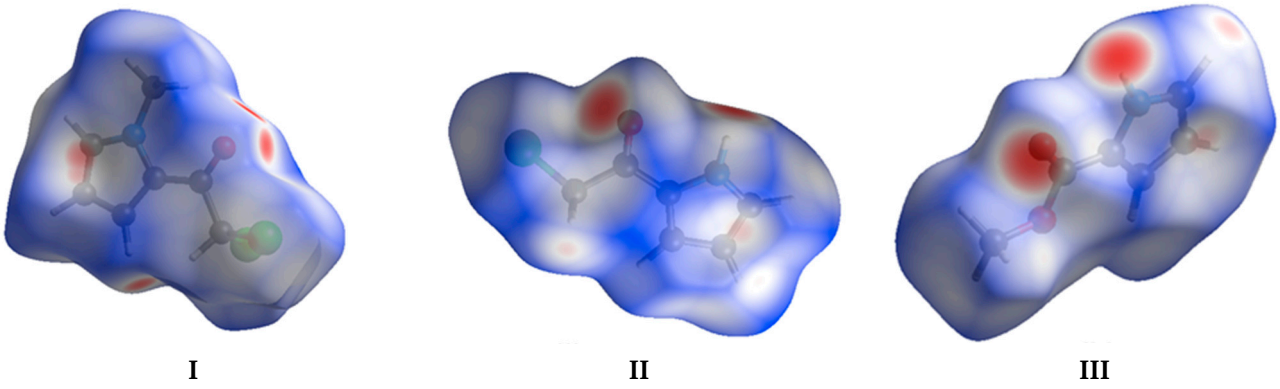

Figure 7. Hirshfeld surfaces of compound **I-III** mapped over d_{norm}.

The fingerprint plots [49,50] presented in Figure 8 show all the molecular interactions, and the most occurring interactions that have been extracted from the Hirshfeld surface.

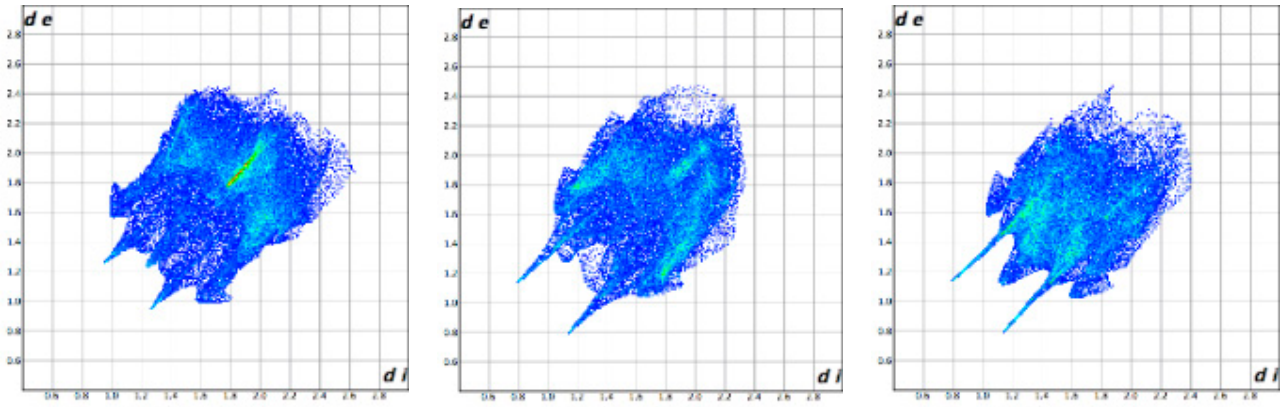

Figure 8. Fingerprint plots of compound **I-III** showing all the interactions taken from the Hirshfeld surface.

The most different types of contacts can be observed for **II**, while **III** has the fewest. The most frequent contacts are H···H, H···C/C···H and H···Cl/Cl···H. The H···H contacts account for 25% to 45% of the total interactions, H···Cl/Cl···H interactions account for 26% to 29%, and H···C/C···H interactions account for 14% to 21% of all interactions. In structure **I**, which features an N-methyl group instead of an H-atom, the share of H···H contacts is about 25% at the expense of H···Cl/Cl···H (29%). For structure **II**, which features one Cl-atom, the shares of H···H, H···Cl/Cl···H interactions are equal at 25% and H···C/C···H interactions account for 20%. In **III**, in which there are no Cl-atoms and a methyl group instead of N-H, H···H contacts account for 45% of the interactions and the share of H···O/O···H interactions is the highest one, at 25%.

It is worth noting that for the H···C/C···H, H···O/O···H contacts, their percentage share does not change drastically between the compounds. It is interesting that compounds **I-II** contain Cl-atoms, and yet the percentage of Cl···Cl interactions is rather low; in the structure with two Cl-atoms, they account for only 8.7% (**I**) and the lowest contribution of the Cl···Cl contacts is in the structure with one Cl-atom, (**II**), which accounts for only 0.4% of the interactions. These interactions are longer than sum of the van der Waals radii, and cannot be recognized as typical halogen bonds (e.g., for **I** the distance is 3.581Å). The graphical representations of the composition of different types of interactions in compound **I-III** are shown in Figure 9, and the fingerprint plots for the most frequently occurring interactions are shown in Table S2.

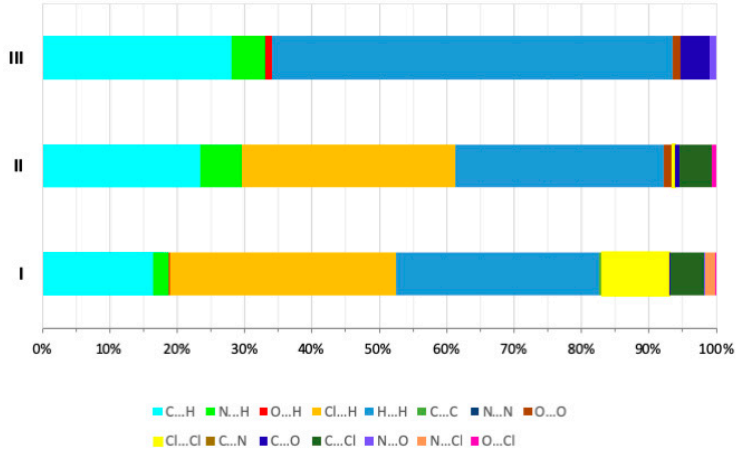

Figure 9. Fingerprint plots of compound **I-III** showing all the interactions taken from the Hirshfeld surface.

4. Conclusions

The crystal and molecular structure of three derivatives of carbonyl 2-substituted pyrroles was determined by the single crystal X-ray diffraction combined with the single point calculations at ωB97XD/6-311++G(d,p) level of theory and descriptive Hirshfeld analysis. All investigated compounds crystallize with one molecule in the asymmetric unit in $P2_12_12_1$, for **I** and **II**, and $P2_1/c$ space group, for **III**. Despite the similar molecular structures of investigated compounds, they feature distinct H-bond motifs in the crystalline phase. In the structure of **I**, the dimers $R_1^2(5)$ and $R_2^1(7)$ created by C-H···O and C-H···Cl bonds form a chain along the **b**-axis. In structures **II** and **III**, C(5) chain motifs are formed. In structure **II**, an infinite chain of N-H···O H-bonds forms along the **a**-axis, and is stabilized by N-H···Cl and C-H···O interactions. Similarly, in structure **III**, N-H···O form a chain along the **b**-axis. Between the chains, weak C-H···O interactions create centrosymmetric dimers, giving the $R_2^2(6)$ motif. Additionally, the 3D network in the structures **I-III** is stabilized by C-H···π interactions. The single point calculations at ωB97XD/6-311++G(d,p) level of theory indicate that the systems with N-H···O bonds (**II** and **III**) have greater interaction energies (**II** 11.02 kcal/mol and **III** 8.36 kcal/mol), compared with the weak C-H···O/Cl H-bonds occurring in structure **I** (7.62 kcal/mol). Hirshfeld analysis showed that in structure **III**, in which there are no chlorine atoms, H···H interactions predominate, accounting for 45% of the total number of intermolecular interactions, while H···O/O···H is 25%. For the compounds with chlorine atoms (**I-II**), H···H similarly accounts for 25%. Furthermore, H···Cl/Cl···H interactions contribute 29% for **I** (with two Cl-atoms) and 25% for **II** (one Cl-atom), whereas H···O/O···H contribute accounting 15% and 18% for **I** and **II**, respectively.

Supplementary Materials: The following supporting information can be downloaded at: https://www.mdpi.com/article/10.3390/cryst12111523/s1, Table S1. Selected geometrical parameters [Å, °] between atoms in non-hydrogen skeleton of molecules; Table S2. Fingerprint plots of compound **I-III** showing the most important interactions occurring in crystals of **I**, **II** and **III** taken from the Hirshfeld surface; Figure S1. Full Interaction Maps for investigated structures **I-III** with interacting molecules; Scheme S1. Scheme of the searching fragment of pyrrol-2-yl ketone; Scheme S2. Scheme of the searching fragment of molecule of ester; Table S3. Values of bond lengths [Å] in the structures of the pyrrol-2-yl ketones derivatives found in CSD; Table S4. Values of bond angles [°] in the structures of the pyrrol-2-yl ketones derivatives found in CSD; Table S5. Values of bond lengths [Å] in the structures of the pyrrol-2-carboxylate derivatives found in CSD; Table S6. Values of bond angles [°] in the structures of the pyrrol-2-carboxylate derivatives found in CSD; Figure S2. Graphical representation of the structures of the pyrrol-2-yl ketones derivatives found in CSD; Figure S3. Graphical representation of the structures of the pyrrol-2-carboxylate derivatives found in CSD.

Author Contributions: Conceptualization, M.D.; methodology, M.D. and A.T.D.; software, M.D., A.T.D., S.W., M.Z.; formal analysis, M.D.; investigation, M.D. and S.W.; writing—original draft preparation, M.D.; writing—review and editing, M.D. and A.P.; visualization, M.D. All authors have read and agreed to the published version of the manuscript.

Funding: This research received no external funding.

Data Availability Statement: Not applicable.

Acknowledgments: Calculations have been carried out using resources provided by the Wroclaw Centre for Networking and Supercomputing (http://wcss.pl (accessed on 21 October 2022)), grant No. 68. Access to HPC machines and licensed software is gratefully acknowledged by M.D.

Conflicts of Interest: The authors declare no conflict of interest.

References

1. Khoury, R.G.; Jaquinod, L.; Nguyen, L.T.; Smith, K.M. Macrocycles containing five pyrrole subunits: The iso-oxopentaphyrin system. *Heterocycles* **1998**, *47*, 113–119. [CrossRef]
2. Tamiaki, H.; Hamada, K.; Kunieda, M. Synthesis of 3/8-carbonylated chlorophyll derivatives and regiodependent reductivity of their carbonyl substituents. *Tetrahedron* **2008**, *64*, 5721–5727. [CrossRef]

3. Rowan, D.D.; Gaynor, D.L. Isolation of feeding deterrents against argentine stem weevil from ryegrass infected with the endophyte Acremonium loliae. *J. Chem. Ecol.* **1986**, *12*, 647–658. [CrossRef] [PubMed]
4. Dubis, E.N.; Brattsten, L.B.; Dungan, L.B. Effects of the endophyte-associated alkaloids peramine on Southern Armworm Microsomal Cytochrome P450. In *ACS Symposium Series Molecular mechanism of Insecticide Resistance Diversity among Insects*; ACS: Washington, DC, USA, 1992.
5. Dubis, A.T.; Łapiński, A. Spectroscopic and theoretical study on peramine and some pyrrolopyrazinone compounds. *Vib. Spec.* **2009**, *49*, 265–273. [CrossRef]
6. Łapiński, A.; Dubis, A.T. A DFT/TD-DFT study for the ground and excited states of peramine and some pyrrolopyrazinone compounds. *J. Phys. Org. Chem.* **2009**, *22*, 1058–1064. [CrossRef]
7. Bellina, F.; Rossi, R. Synthesis and biological activity of pyrrole, pyrroline and pyrrolidine derivatives with two aryl groups on adjacent positions. *Tetrahedron* **2006**, *62*, 7213–7256. [CrossRef]
8. Snavely, D.L.; Blackburn, F.R.; Ranasinghe, Y.; Walters, V.A.; Gonzalez del Riego, M. Vibrational overtone spectroscopy of pyrrole and pyrrolidine. *J. Phys. Chem.* **1992**, *96*, 3599–3605. [CrossRef]
9. Lukeš, V.; Breza, M.; Biskupič, S. Interaction energy anisotropy of the pyrrole dimer: Ab initio theoretical study. *Theor. Chem. Acc.* **1999**, *101*, 319–324. [CrossRef]
10. Dunbar, R.C. Binding of Na^+, Mg^+, and Al^+ to the π Faces of Naphthalene and Indole: Ab Initio Mapping Study. *J. Phys. Chem. A* **1998**, *102*, 8946–8952. [CrossRef]
11. Pullman, A.; Berthier, G.; Savinelli, R. Theoretical study of binding of tetramethylammonium ion with aromatics. *J. Comput. Chem.* **1997**, *18*, 2012–2022. [CrossRef]
12. Pullman, A.; Berthier, G.; Savinelli, R. Interaction of the tetramethylammonium ion with the cycles of aromatic amino acids beyond the SCF ab initio level. *J. Am. Chem. Soc.* **1998**, *120*, 8553–8554. [CrossRef]
13. Farnier, M.; Drakenberg, T. Nuclear magnetic resonance conformational studies of C-substituted pyrrolecarbaldehydes. Part, I. Substituent effects on aldehyde conformations as shown by long range coupling constants. *J. Chem. Soc. Perkin Trans.* **1975**, *2*, 333–337. [CrossRef]
14. John, I.G.; Ritchie, G.L.D.; Radom, L. Conformations of Furan-, Pyrrole-, and Pyridine-carbaldehydes: An Ab Initio Molecular Orbital Study. *J. Chem. Soc. Perkin Trans.* **1977**, *2*, 1601–1607. [CrossRef]
15. Farnier, M.; Drakenberg, T. Nuclear magnetic resonance conformational studies of C-substituted pyrrolecarbaldehydes. Part II. Barrier to internal rotation in 5-substituted pyrrole-2-carbaldehydes. *J. Chem. Soc. Perkin Trans.* **1975**, *2*, 337–340. [CrossRef]
16. Dubis, A.T.; Grabowski, S.J. Infrared spectroscopic and theoretical ab initio studies on conformational isomers of methyl pyrrole-2-carboxylate. *J. Mol. Struct.* **2001**, *562*, 107–117. [CrossRef]
17. Dubis, A.T.; Grabowski, S.J. Spectroscopic and theoretical studies on the monomeric and dimeric forms of methyl pyrrole-2-carboxylate. *New J. Chem.* **2002**, *26*, 165–169. [CrossRef]
18. Dubis, A.T.; Grabowski, S.J. Infrared, Density-Functional Theory, and Atoms in Molecules Method Studies on Conformers of Some 2-Substituted 1H-Pyrroles. *J. Phys. Chem. A* **2003**, *107*, 8723–8729. [CrossRef]
19. Grabowski, S.J.; Dubis, A.T.; Martynowski, D.; Glówka, M.; Palusiak, M.; Leszczynski', J. Crystal and molecular structure of pyrrole-2-carboxylic acid; pi-Electron delocalization of its dimers-DFT and MP2 calculations. *J. Phys. Chem. A* **2004**, *108*, 5815–5822. [CrossRef]
20. Balaban, A.T.; Oniciu, D.C.; Katritzky, A.R. Aromaticity as a cornerstone of heterocyclic chemistry. *Chem. Rev.* **2004**, *104*, 2777–2812. [CrossRef]
21. Alkorta, I.; Elguero, J. How Aromaticity Affects the Chemical and Physicochemical Properties of Heterocycles: A Computational approach in Aromaticity in Heterocyclic Compounds. In *Topics in Heterocyclic Chemistry*; Krygowski, T.M., Cyrański, M.K., Eds.; Springer: Berlin/Heidelberg, Germany, 2009; Volume 19, pp. 155–202.
22. Dubis, A.T.; Wojtulewski, S.; Filipkowski, K. Spectroscopic and theoretical studies on the aromaticity of pyrrol-2-yl-carbonylconformers. *J. Mol. Struct.* **2013**, *1041*, 92–99. [CrossRef]
23. Desiraju, R.; Steiner, T. The Weak Hydrogen Bond. In *Structural Chemistry and Biology*; Oxford University Press, Inc.: New York, NY, USA, 1999. [CrossRef]
24. Desiraju, G.R. *Crystal Engineering: The Design of Organic Solids*; Elsevier: Amsterdam, The Netherlands, 1989. [CrossRef]
25. Price, S.L.; Stone, A.J.; Lucas, J.; Rowland, R.S.; Thornley, A.E. The nature of -Cl$\cdots$Cl- intermolecular interactions. *J. Am. Chem. Soc.* **1994**, *116*, 4910–4918. [CrossRef]
26. Metrangolo, P.; Resnati, G. Halogen bonding: A paradigm in supramolecular chemistry. *Chem. Eur. J.* **2001**, *7*, 2511–2519. [CrossRef]
27. Day, G.M.; Price, S.L. A Nonempirical Anisotropic Atom-Atom Model Potential for Chlorobenzene Crystals. *J. Am. Chem. Soc.* **2003**, *125*, 16434–16443. [CrossRef] [PubMed]
28. Formigué, M.; Batail, P. Activation of hydrogen- and halogen-bonding interactions in tetrathiafulvalene-based crystalline molecular conductors. *Chem. Rev.* **2004**, *104*, 5379–5418. [CrossRef]
29. Zordan, F.; Brammer, L.; Sherwood, P. Supramolecular chemistry of halogens: Complementary features of inorganic (M-X) and organic (C-X′) halogens applied to M-X$\cdots$X′-C halogen bond formation. *J. Am. Chem. Soc.* **2005**, *127*, 5979–5989. [CrossRef] [PubMed]

30. Politzer, P.; Murray, J.S.; Clark, T. Halogen bonding: An electrostatically-driven highly directional noncovalent interaction. *Phys. Chem. Chem. Phys.* **2010**, *12*, 7748–7757. [CrossRef]
31. Legon, A.C. The halogen bond: An interim perspective. *Phys. Chem. Chem. Phys.* **2010**, *12*, 7736–7747. [CrossRef]
32. Bilewicz, E.; Rybarczyk-Pirek, A.; Dubis, A.T.; Grabowski, S.J. Halogen bonding in crystal structure of 1-methylpyrrol-2-yl trichloromethyl ketone. *J. Mol. Struct.* **2007**, *829*, 208–211. [CrossRef]
33. Dubis, A.; Grabowski, S.J.; Romanowska, D.B.; Misiaszek, T.; Leszczynski, J. Pyrrole-2-carboxylic Acid and Its Dimers: Molecular Structures and Vibrational Spectrum. *J. Phys. Chem. A* **2002**, *106*, 10613–10621. [CrossRef]
34. Etter, M.C. Encoding and decoding hydrogen-bond patterns of organic compounds. *Acc. Chem. Res.* **1990**, *23*, 120–126. [CrossRef]
35. Etter, M.C.; Bernstein, J.B.; McDonald, J.C. Graph-set analysis of hydrogen-bond patterns in organic crystals. *Acta Crystallogr. Sect. B Struct. Sci.* **1990**, *46*, 256–262. [CrossRef] [PubMed]
36. Santos, A.F.L.O.M.; Riberio da Silva, M.A.V. Experimental and Computational Study on the Molecular Energetics of 2-Pyrrolecarboxylic Acid and 1-Methyl-2-pyrrolecarboxylic Acid. *J. Phys. Chem. A* **2009**, *113*, 9741–9750. [CrossRef] [PubMed]
37. Groom, C.R.; Bruno, I.J.; Lightfoot, M.P.; Ward, S.C. The Cambridge Structural Database. *Acta Crystallogr. Sect. B* **2016**, *72*, 171–179. [CrossRef]
38. Nicolau, I.; Demopoulus, V.J. A study of the friedel-crafts acylation of 1-benzenesulfonyl-1H-pyrrole in the preparation of 3-aroylpyrroles. *J. Heterocycl. Chem.* **1998**, *35*, 1345–1348. [CrossRef]
39. Dubis, A.T.; Domagała, M.; Grabowski, S.J. Spectroscopic and theoretical studies on some new pyrrol-2-yl-chloromethyl ketones. *New J. Chem.* **2010**, *34*, 556–566. [CrossRef]
40. Bailey, D.M.; Johnson, R.E.; Albertson, N.F. Ethyl pyrrole-2-carboxylate. *Org. Synth.* **1971**, *51*, 100–104. [CrossRef]
41. *STOE IPDS-Software*, Version 2.89; STOE & CIE GmbH: Darmstadt, Germany, 1998.
42. North, A.C.T.; Phillips, D.C.; Mathews, F.S. A semi-empirical method of absorption correction. *Acta Cryst. A* **1968**, *24*, 351–359. [CrossRef]
43. Clark, R.C.; Reid, J.S. The analytical calculation of absorption in multifaceted crystals. *Acta Cryst. A* **1995**, *51*, 887–897. [CrossRef]
44. Altomare, A.; Burla, M.C.; Camalli, M.; Cascarano, G.L.; Giacovazzo, C.; Guagliardi, A.; Moliterni, A.G.G.; Polidori, G.; Spagna, R. SIR97: A new tool for crystal structure determination and refinement. *J. Appl. Cryst.* **1999**, *32*, 115–119. [CrossRef]
45. Sheldrick, G.M. A short history of SHELX. *Acta Cryst. A* **2008**, *64*, 112–122. [CrossRef]
46. Sheldrick, G.M. Crystal structure refinement with SHELXL. *Acta Cryst. C* **2015**, *71*, 3–8. [CrossRef] [PubMed]
47. Spek, A.L. Structure Validation in chemical crystallography. *Acta Cryst. D* **2009**, *65*, 148–155. [CrossRef] [PubMed]
48. Macrae, C.F.; Sovago, I.; Cottrell, S.J.; Galek, P.T.A.; McCabe, P.; Pidcock, E.; Platings, M.; Shields, G.P.; Stevens, J.S.; Towler, M.; et al. Mercury 4.0: From visualization to analysis, design and prediction. *J. Appl. Cryst.* **2020**, *53*, 226–235. [CrossRef] [PubMed]
49. Turner, M.J.; McKinnon, J.J.; Wolff, S.K.; Grimwood, D.J.; Spackman, P.R.; Jayatilaka, D.; Spackman, M.A. *CrystalExplorer17*; University of Western Australia: Perth, Australia, 2017.
50. Spackman, M.A.; Jayatilaka, D. Hirshfeld surface analysis. *CrystEngComm* **2009**, *11*, 19–32. [CrossRef]
51. Chai, J.-D.; Head-Gordon, M. Long-range corrected hybrid density functionals with damped atom–atom dispersion corrections. *Phys. Chem. Chem. Phys.* **2008**, *10*, 6615–6620. [CrossRef] [PubMed]
52. McLean, A.D.; Chandler, G.S. Contracted Gaussian basis sets for molecular calculations. I. Second row atoms, Z=11–18. *J. Chem. Phys.* **1980**, *72*, 5639–5648. [CrossRef]
53. Frisch, M.J.; Pople, J.A.; Binkley, J.S. Self-consistent molecular orbital methods 25. Supplementary functions for Gaussian basis sets. *J. Chem. Phys.* **1984**, *80*, 3265–3269. [CrossRef]
54. Krishnan, R.; Binkley, J.S.; Seeger, R.; Pople, J.A. Self-consistent molecular orbital methods. XX. A basis set for correlated wave functions. *J. Chem. Phys.* **1980**, *72*, 650–654. [CrossRef]
55. Clark, T.; Chandrasekhar, J.; Spitznagel, G.W.; Schleyer, P.V.R. Efficient diffuse function-augmented basis sets for anion calculations. III.† The 3-21+G basis set for first-row elements, Li–F. *J. Comput. Chem.* **1983**, *4*, 294–301. [CrossRef]
56. Domagała, M.; Lutyńska, A.; Palusiak, M. Extremely Strong Halogen Bond. The Case of a Double-Charge-Assisted Halogen Bridge. J. *Phys. Chem. A* **2018**, *122*, 5484–5492. [CrossRef]
57. Domagała, M.; Matczak, P.; Palusiak, M. Halogen bond, hydrogen bond and N···C interaction—On interrelation among these three noncovalent interactions. *Comput. Theor. Chem.* **2012**, *998*, 26–33. [CrossRef]
58. Allen, F.H.; Bruno, I.J. Bond lengths in organic and metal-organic compounds revisited: *X*—H bond lengths from neutron diffraction data. *Acta Crystallogr. B* **2010**, *66*, 380–386. [CrossRef] [PubMed]
59. Frisch, M.J.; Trucks, G.W.; Schlegel, H.B.; Scuseria, G.E.; Robb, M.A.; Cheeseman, J.R.; Scalmani, G.; Barone, V.; Mennucci, B.; Petersson, G.A.; et al. *Gaussian 09, Revision, D.01*; Gaussian, Inc.: Wallingford, CT, USA, 2013.
60. Boys, S.F.; Bernardi, F. The calculation of small molecular interactions by the differences of separate total energies. Some procedures with reduced errors. *Mol. Phys.* **1970**, *19*, 553–566. [CrossRef]
61. Grabowski, S.J.; Dubis, A.T.; Palusiak, M.; Leszczyński, J. Heteronuclear Intermolecular Resonance-Assisted Hydrogen Bonds. The Structure of Pyrrole-2-Carboxamide (PyCa). *J. Phys. Chem. B* **2006**, *110*, 5875–5882. [CrossRef]
62. Kerscher, T.; Mayer, P.; Klufers, P. Methyl 1*H*-pyrrole-2-carboxylate. *Acta Cystallogr. Sect. E Struct. Rep. Online* **2009**, *65*, o2195. [CrossRef]

63. Essa, A.H.; Lerrick, R.I.; Ciftci, E.; Harrington, R.W.; Waddell, P.G.; Clegg, W.; Hall, M.J. Grignard-mediated reduction of 2,2,2-trichloro1-arylethanones. *Org. Biomol. Chem.* **2015**, *13*, 5793. [CrossRef]
64. Putz, H.; Brandenburg, K. Diamond—Crystal and Molecular Structure Visualization. Version 4.6.4, Bonn, Germany. Available online: https://www.crystalimpact.de/diamond (accessed on 15 December 2020).
65. Grimme, S. Semi-empirical GGA-type density functional constructed with a long-range dispersion correction. *J. Comput. Chem.* **2006**, *27*, 1787–1799. [CrossRef]
66. Scheiner, S. Weak H-bonds. Comparisons of CH$\cdots$O to NH$\cdots$O in proteins and PH$\cdots$N to direct P$\cdots$N interactions. *Phys. Chem. Chem. Phys.* **2011**, *13*, 13860–13872. [CrossRef]